Available online at www.sciencedirect.com

ScienceDirect

Mendeleev Commun., 2020, **30**, 534–536

Mendeleev Communications

Phase diagram of the water–monoethanolamine system

Yuri P. Klapshin,[a] Irina A. Solonina,[b] Margarita N. Rodnikova,*[b] Mikhail R. Kiselev,[c] Andrey V. Khoroshilov[b] and Sergey V. Makaev[d]

[a] *N. I. Lobachevsky Nizhny Novgorod State University, 603950 Nizhny Novgorod, Russian Federation*
[b] *N. S. Kurnakov Institute of General and Inorganic Chemistry, Russian Academy of Sciences, 119991 Moscow, Russian Federation. E-mail: rodnikova@igic.ras.ru*
[c] *A. N. Frumkin Institute of Physical Chemistry and Electrochemistry, Russian Academy of Sciences, 119071 Moscow, Russian Federation*
[d] *A. V. Topchiev Institute of Petrochemical Synthesis, Russian Academy of Sciences, 119991 Moscow, Russian Federation*

DOI: 10.1016/j.mencom.2020.07.044

DSC and DTA were used to construct the phase diagram of the water–monoethanolamine (MEA) system in a temperature range of 133–313 K. The phase diagram is characterized by the supercooling of a liquid phase and devitrification at ~150 K. MEA·2H_2O (congruently melted at 238 K), MEA·H_2O (incongruently melted at 248 K), and limited solid solutions of MEA in H_2O were detected.

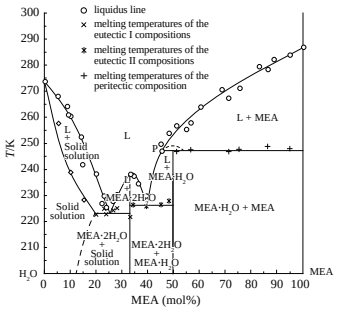

Keywords: monoethanolamine (ethanolamine), water, phase diagram, differential scanning calorimetry, differential thermal analysis.

Monoethanolamine (MEA) is miscible with water in any ratios, and both of the solvents and their solutions have spatial H-bond networks. A higher electron-donating ability and a larger dipole moment of the MEA molecule in comparison with water should be noted. However, the energies of intermolecular H-bonds in these compounds are close. Unlike water, MEA molecules have intramolecular H-bonds in both gas[1,2] and liquid phases, and they form ten conformers.[3] A *gauche* conformer, where the intramolecular bond is supported by the O–C–C–N dihedral angle, is the most stable conformer. The *gauche* conformer is typical of MEA in gas and liquid phases,[4] while the *trans* conformer is typical of a crystalline phase.[5,6] The densities of liquid water and MEA are similar, whereas the viscosity of MEA is about 20 times higher due to the unique mobility of the water molecule.[7]

The investigation of solvent systems with H-bonds in a solid phase is important because the presence of a three-dimensional network of hydrogen bonds can explain the supercooling of a liquid phase in these systems, the difficulty of their crystallization, and the ease of vitrification. These properties are essential for the preservation of living organisms,[8–12] and aqueous MEA solutions are widely used in cryobiology.[13–16] Therefore, we studied the phase diagram of the H_2O–MEA system by differential scanning calorimetry (DSC) and differential thermal analysis (DTA). Previously,[13,14] this phase diagram was examined in narrow temperature and concentration ranges.[†]

Table 1 summarizes the results obtained by DTA and DSC, and Figure 1 shows the DTA curves of crystallized H_2O–MEA mixtures (DTA peaks correspond to the phase transition temperatures given in Table 1).

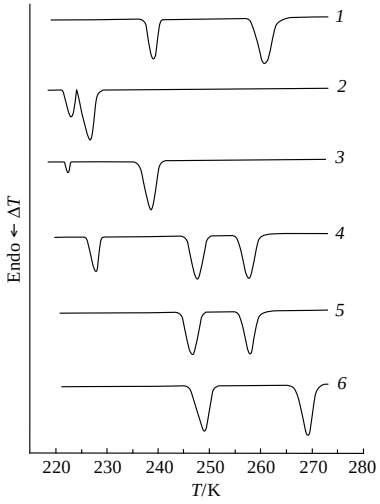

Figure 1 DTA curves of the H_2O–MEA system at MEA concentrations of (*1*) 9.9, (*2*) 23.7, (*3*) 32.1, (*4*) 44.9, (*5*) 51.0 and (*6*) 71.0 mol%.

[†] The solutions of MEA (99%, Acros) without additional purification in water, which was purified with Milli-Q, were prepared gravimetrically. A DTA system[17] developed at the University of Nizhny Novgorod and a Q100 DSC instrument (TA Instruments) were used for measurements with cooling from 298 to 183 K and heating (183–313 K) at a rate of 3 K min^{-1} in a stream of high purity argon. The temperature error was ± 1 °C. A Mettler TA4000 system was used in the DSC30 mode with rapid sample cooling in liquid nitrogen (298–133 K) and the subsequent heating at a rate of 3 K min^{-1} (133–313 K). The data were collected only during the heating of cooled samples. The error in temperature measurements did not exceed ±5 °C.

Table 1 Phase transition temperatures in the H_2O–MEA system.

MEA (mol%)	Temperature/K							
	liquidus	solidus	eutectic I	eutectic II	peritectic	crystallization I	crystallization II	devitrification
0.00	273	–	–	–	–	–	–	–
5.08	268	258	–	–	–	–	–	–
5.73	270	–	–	–	–	257	–	–
8.70	264	–	–	–	–	–	–	153
9.03	261	–	–	–	–	249	–	–
9.91	261	239	–	–	–	–	–	–
14.49	242	-	–	–	–	205	–	–
15.07	250	229	–	–	–	–	–	–
19.90	238	–	223	–	–	–	–	–
22.10	227	–	–	–	–	–	–	151
22.92	230	–	225	–	–	–	–	–
23.71	226	–	223	–	–	–	–	–
26.35	228	–	225	–	–	–	–	–
27.93	231	–	225	–	–	–	–	–
32.31	–	–	–	–	–	–	–	154
33.05	238	–	222	–	–	–	–	–
33.20	–	–	–	–	–	236	261	–
34.21	238	–	–	227	–	–	–	–
36.09	235	–	–	–	–	–	–	–
37.52	–	–	–	–	–	–	–	156
37.90	240	–	–	–	–	219	263	–
39.21	230	–	–	226	–	–	–	–
44.93	250	–	–	227	247	–	–	–
48.00	254	–	–	228	248	–	–	–
50.21	–	–	–	–	–	–	–	158
50.98	257	–	–	–	247	–	–	–
54.69	256	–	–	–	–	–	–	160
56.44	258	–	–	–	248	–	–	–
60.15	264	–	–	–	–	–	–	–
70.43	278	–	–	–	–	229	–	–
71.07	268	–	–	–	246	–	–	–
75.37	271	–	–	–	248	–	–	–
82.98	280	–	–	–	–	236	–	–
86.13	279	–	–	–	249	–	–	–
88.64	282	–	–	–	–	246	–	–
94.70	284	–	–	–	248	–	–	–
100.00	287	–	–	–	-	246	–	–

The thermograms recorded on the cooling of samples manifest exothermic peaks due to crystallization from the supercooled samples. The supercooling effect varies from 20 to 40 K for different compositions.

On the rapid cooling of samples, they vitrified, and the thermograms showed a drop of the baseline at 150–160 K upon heating at a rate of 3 K min^{-1}, which was attributed to the transition of a glass to a supercooled liquid. The subsequent heating led to exothermic peaks due to the crystallization of supercooled liquid and endothermic peaks due to the melting of crystallized samples.

Three isotherms (including two eutectics) were found in the test system. Eutectic I appeared at 223 K in a concentration range of 18–33 mo% MEA with an eutectic point at 24 mol% MEA. Eutectic II was observed at 228 K in a concentration range of 33–50 mol% MEA with an eutectic point at 39 mol% MEA. The third line is a peritectic (P) at a temperature of 248 K, which characterizes incongruent melting with the decomposition of a solid hydrate ($MEA{\cdot}H_2O$) to a solution containing 45 mol% MEA and solid MEA. Thus, the MEA–H_2O system has a MEA dihydrate that congruently melts at 238 K and a MEA monohydrate that incongruently melts at 248 K. In a concentration range of 5–18%, MEA forms a solid solution with water.

A phase diagram of the H_2O–MEA system was constructed using the phase transition equilibriums (Figure 2).

Thus, we used DTA and DSC to study the phase diagram of the H_2O–MEA system. A MEA dihydrate congruently melting at 238 K and a MEA monohydrate melting at 248 K were detected.

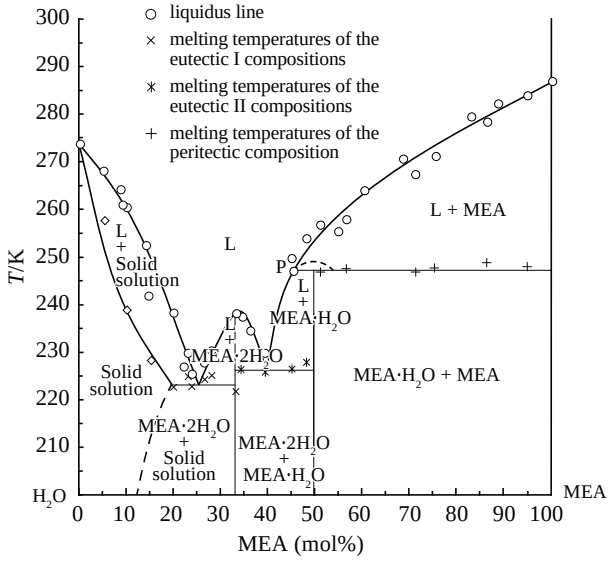

Figure 2 Phase diagram of the H_2O–MEA system.

The immersion of H_2O–MEA samples in liquid nitrogen led to vitrification, while cooling the samples at a rate of 3 K min^{-1} led to supercooling. The strong supercooling of a liquid phase and a tendency of the system to undergo glass transition were determined by the stability of a mixed spatial network of hydrogen bonds in the H_2O–MEA system.

This study was carried out at N. S. Kurnakov Institute of General and Inorganic Chemistry of the Russian Academy of Sciences and supported by the Russian Foundation for Basic Research (project no. 19-03-00215).

References

1 I. Vorobyov, M. C. Yappert and D. B. DuPre, *J. Phys. Chem. A*, 2002, **106**, 668.
2 C. F. P. Silva, M. L. T. S. Duarte and R. Fausto, *J. Mol. Struct.*, 1999, **482**–**483**, 591.
3 Yu. V. Novakovskaya and M. N Rodnikova, *Dokl. Phys. Chem*., 2016, **467**, 60 (*Dokl. Akad. Nauk*, 2016, **467**, 679).
4 Yu. V. Novakovskaya and M. N. Rodnikova, *Struct. Chem.*, 2015, **26**, 177.
5 M. N. Rodnikova, I. A. Solonina, A. B. Solovei and T. M. Usacheva, *Russ. J. Inorg. Chem.*, 2013, **58**, 1501 (*Zh. Neorg. Khim.*, 2013, **58**, 1628).
6 D. Mootz, D. Brodalla and M. Wiebcke, *Acta Crystallogr.*, 1989, **C45**, 754.
7 M. N. Rodnikova, G. M. Agayan and N. K. Balabaev, *J. Mol. Liq.*, 2019, **283**, 374.
8 J. S. Clegg, *Comp. Biochem. Physiol., Part B: Biochem. Mol. Biol*., 2001, **128**, 613.
9 E. Shalaev and F. Franks, in *Amorphous Food and Pharmaceutical Systems*, ed. H. Levine, RSC Publishing, Cambridge, UK, 2002, pp. 200–215.
10 M. P. Buera, Y. Roos, H. Levine, L. Slade, H. R. Corti, D. S. Reid, T. Auffret and C. A. Angell, *Pure Appl. Chem*., 2011, **83**, 1567.
11 L. Slade and H. Levine, *Crit. Rev. Food Sci. Nutr.*, 1991, **30**, 115.
12 I. A. Solonina, M. N. Rodnikova, M. R. Kiselev, A. V. Khoroshilov and S. V. Makaev, *Mendeleev Commun.*, 2019, **29**, 693.
13 P. M. Mehl, *Thermochim. Acta*, 1993, **226**, 325.
14 A. Baudot, C. Cacela, M. L. Duarte and R. Fausto, *Cryobiology*, 2002, **44**, 150.
15 L. Luo, Y. Pang, Q. Chen and G. Li, *CryoLetters*, 2006, **27**, 341.
16 V. I. Grischenko, *Problemy Kriobiologii*, 2005, **15**, 231 (in Russian).
17 I. A. Korshunov and Yu. P. Klapshin, *Trudy po Khimii i Khim. Tekhnologii / Gor'kovskii Gos. Universitet*, 1968, no.1, 3 (in Russian).

Received: 12th December 2019; Com. 19/6088